Energy Fuels **XXXX,** *XXX,* 000–000 · DOI:10.1021/ef100882t

energy&fuels
article

Changes in the Structure of the Cellulose Fiber Wall during Dilute Acid Pretreatment in *Populus* Studied by ^{1}H and ^{2}H NMR

Marcus Foston and Arthur J. Ragauskas*

BioEnergy Science Center, School of Chemistry and Biochemistry, Institute of Paper Science and Technology, Georgia Institute of Technology, 500 10th Street, Atlanta, Georgia 30332

Received October 28, 2009. Revised Manuscript Received August 30, 2010

Dilute acid pretreatment (DAP) is a frequently employed technique in biofuel production to increase overall sugar and subsequent ethanol yields from downstream fermentation. This is done prior to enzymatic deconstruction of cellulose to increase accessible surface area as well as to remove or redistribute hemicellulose and lignin, which have an inhibitory effect on enzymatic hydrolysis. In this study, the effect of DAP on the supramolecular and ultrastructure of lignocellulosic biomass was evaluated by both ^{1}H and ^{2}H NMR techniques. A series of DAPs were conducted on *Populus* using ~0.10 M H_2SO_4 at ~160 °C for varying residence times. ^{2}H spin−lattice (T_1) times of deuterium oxide (D_2O) adsorbed within the lignocellulosic biomass were measured on untreated and pretreated *Populus*, and an inverse Laplace transform of the T_1 decays was then used to generate pore size distributions. The resulting distributions indicate that substantial pore expansion within the cellulose fibril bundles occurs during pretreatment. ^{1}H Goldman−Shen (GS) spin−diffusion experiments which were also conducted, qualitatively supporting the magnitude of observed pore expansion obtained from ^{2}H NMR relaxation profiles. ^{1}H Carr−Purcell−Meiboom−Gill (CPMG) and pulse field gradient (PFG) experiments were used to investigate the altering supramolecular structure of the lignocellulose and the self-diffusive behavior of water adsorbed within the biomass as a function of DAP. Spin−spin (T_2) relaxation times indicate the nature of cellulose−water interactions change during DAP. Inverse Laplace distributions of the resulting T_2 decays demonstrate not only a shift in T_2 times to longer relaxation or a more mobile state but also indicate that the population of water with longer relaxation times increase, indicating that pretreatment begins to break down and loosen the cellulosic ultrastructure within the biomass. Lastly, the water self-diffusion experiments demonstrates that DAP increases pore tortuosity within the biomass.

1. Introduction

Lignocellulosic biomass is a complex microstructured material composed of varying proportions of lignin and hemicellulose forming a matrix encapsulating and supporting cellulose fibrils packed into bundles.[1] Nature purposefully designed the microstructure of the biopolymers within lignocellulose to serve as a structural component within the cell walls of plants and microorganisms, as a consequence making many biomass sources difficult to deconstruct.[2] High yield, low-cost, and effective deconstruction of cellulose, typically by enzymatic hydrolysis, are the most critical barriers to widespread use of renewable energy sources, such as second generation biofuels, e.g., cellulosic ethanol.[2,3]

The efficiency of enzymatic hydrolysis is directly related to cellulase enzyme activity and the potential effect of substrate characteristics, such as crystallinity, degree of polymerization, specific surface area, and the lignin/hemicellulose distribution.[4−6] Accessible surface area has been identified as a particularly important factor in the rate of enzymatic deconstruction, particularly in the early stages of the hydrolysis.[6] Essentially, increasing the accessible surface area increases the amount of cellulase that can bind to the cellulosic substrate, effectively increasing the hydrolysis rate.

The critical role pore size and the enzyme's ability to diffuse within those pores is particularly highlighted in research by Tanaka et al.[7] Their work on the relationship between pore size and enzyme activity led to a hypothesis that suggests when small pores dominate the pore system, the smaller enzyme components can diffuse into the pores and become trapped there. However, the enzymes become inactive since synergistic interactions with the larger components of the enzyme are no longer possible. Whereas, when larger pores characterize the pore distribution, the entire enzyme can diffuse into and out of the pores and the resulting enzymatic hydrolysis will increase.[7] This was supported by the direct measurement of enzymatic hydrolysis on stream explosion treated mixed hardwood, having a major percentage of pores with a radii of 20 Å or smaller, by purified, partially purified free cellulase (reported if spherical having a radii of 12−38 Å)[8−11] and cross-linked cellulase (to simulate a larger enzyme).[7]

*To whom correspondence should be addressed. Telephone: +1-404-894-9701. Fax: +1-404-894-4778. E-mail: Art.Ragauskas@chemistry.gatech.edu.

(1) Fengel, D., Wegener, G. *Wood: Chemistry, Ultrastructure, Reaction*; Walter de Gruyter: New York, 1984.
(2) Stocker, M. *Angew. Chem., Int. Ed.* **2008**, *47*, 2–14.
(3) Pu, Y.; Zhang, D.; Singh, P. M.; Ragauskas, A. J. *Biofuels, Bioprod. Bioref.* **2008**, *2*, 58–73.
(4) Kumar, R.; Singh, S.; Singh, O. *J. Ind. Microbiol. Biotechnol* **2008**, *35*, 377–391.
(5) Mansfield, S.; Mooney, C.; Saddler, J. *Biotechnol. Prog.* **1999**, *15*, 804–816.
(6) Fan, L. T.; Lee, Y. H.; Beardmore, D. *Biotechnol. Bioeng.* **1980**, *XXII*, 177–I99.
(7) Tanaka, M.; Ikesaka, M.; Matsuno, R.; Converse, A. *Biotechnol. Bioeng.* **1988**, *32*, 698–706.
(8) Ishizawa, C.; Davis, M.; Schell, D.; Johnson, D. *J. Agric. Food Chem.* **2007**, *55*, 2575–2581.

Enzymatic hydrolysis and fermentation to ethanol is typically preceded by pretreatment.[3] The goal of this pretreatment is to reduce the recalcitrance of biomass. This is accomplished by chemically altering the structure of cellulose, hemicellulose, and lignin. In addition, pretreatments open the lignocellulosic matrix and disrupt the crystalline structure of cellulose. During this process, lignin is redistributed and the majority of the hemicellulose is removed, greatly altering the pore size distribution and the accessible surface area.[12−16] The resulting effect of pretreatment is observed as an increased rate of enzymatic hydrolysis.

Native wood fibers for biofuel production are a porous material which can absorb water, enzymes, and other molecular components due to its complex microstructure. For example, there are pores in which water can be found as bound water on and/or within cellulose fibril surfaces or amorphous regions, this water is typically referred to as nonfreezing water. Pore size distributions for hardwoods have been determined by solute exclusion experiments using dextran solutes ranging from 38 to 560 Å in diameter, and this study showed a wide pore diameter distribution, on the order of ∼0.15−50 nm, corresponding to a total specific surface area, specific surface area available to a diameter of 38 Å, and specific surface area available to a diameter of 51 Å of ∼1577, 26, and 14 m^2/g, respectively.[17]

Differential scanning calorimeter (DSC) experiments conducted by Maloney et al. on cellulose fibers containing water distinguished two separate fractions of water having different freezing properties within the fiber wall. Water within 1−3 monolayers of surface hydroxyl groups are said not to freeze because of sufficiently high electrostatic or hydrogen bonding forces which orient the water molecules in an icelike configuration in which their motion is so retarded that formation of ice crystals becomes impossible, hence the term nonfreezing water.[18]

The other water fraction detected by Maloney was water with a depressed freezing point, whose endotherm could not be resolved from that of bulk water, which results from free water confined within pores and/or interacting with fibril surfaces. As the moisture content of the cellulose fiber was changed, the proportion of the two water fractions changed as well as the magnitude of the freezing point depression. This indicated as water is removed, various pore systems of different sizes or pools of water were being accessed. The water corresponding to the water with a depressed freezing point was then described to be "free" water between cellulose fibrils, within voids in the lignocellulosic matrix, and in lumens or capillaries.[18]

Proton relaxation studies support the conclusions made by the DSC experiments. Spin−spin (T_2) relaxation of water adsorbed in western red cedar and Douglas fir sapwood could be described by a distinct three-component decay.[19,20] Water at the surface and between cellulose fibrils was assigned to the fastest relaxing component, water interacting within the lignocellulosic matrix was identified as the component with the medium rate of decay, and the slowest relaxing component was shown to be free water in lumens or capillaries. The relative intensities of each component changed with increasing moisture content, again suggesting as water is added, various pools of water within the pore system are being accessed, presumably starting with the smaller pores.[19]

Topgaard et al. used similar proton relaxation and pulse field gradient (PFG) experiments designed to probe the self-diffusion behavior of water within the biomass to study changes in cellulose fiber wall structure during drying. Along with previous NMR studies, conclusions made via DSC and solute size exclusion experiments by other researchers Topgaard concluded the sequence of water removal for saturated lignocellulosic biomass is (1) bulk water from lumens or capillaries, (2) water in micrometer-scale pores localized in the lignocellulosic matrix, and (3) water in nanometer-scale pores on and between cellulose fibrils. They determined the first pool of water or bulk water disappears below 70−80% moisture content (MC), the second pool is removed at a MC below 20−30%, and the third below 10% MC.[18,21−23] Figure 1 is a schematic displaying the water pools or pore systems in biomass, which are accessed as a function of moisture content.

The characterization of pore sizes and the distribution of pore sizes is important for an understanding of how accessible surface area changes during various treatments and the subsequent effect on enzymatic hydrolysis. Solute size exclusion is one of the most common techniques for determination of pore size distribution in lignocellulosic biomass.[24] In this technique, pore sizes are probed based on macromolecular accessibility and essentially a series of dextrans of different hydrodynamic volumes is added to the biomass. The amount of dextran leaving the solution indicates the relative proportion of pores having a minimal volume equaling that of the dextran molecule. However, this technique does not consider whether dextrans are absorbed to the surface of the biomass or if irregular shaped pores or a highly tortuous pore system has different accessibility characteristics. These limitations can be overcome by an alternative technique that utilizes NMR of a solvent probe.[25,26] Basically H_2O or D_2O has a vastly different T_1 relaxation within the 1−3 monolayers of nonfreezing water than bulk H_2O. The NMR signal from the probe solvent can then be used to determine the pore volume to surface area ratio and the pore size distribution.

In this study, we present for the first time the use of ^1H and ^2H NMR to evaluate the changes occurring in the supramolecular and ultrastructure of lignocellulosic during DAPs via a solvent probe, water. Water can be found spatially localized throughout the lignocellulosic sample, and with dependence on the moisture content, control can be had over the particular

(9) Cowling, E.; Kirk, T. *Biotechnol. Bioeng. Symp.* **1976**, *6*, 95.
(10) Grethlein, H.; Allen, D.; Converse, A. *Biotechnol. Bioeng.* **1984**, *26*, 1498.
(11) Grethlein, H. *BioTechnology* **1985**, *3*, 155.
(12) Soderstrom, J.; Galbe, M.; Zacchi, G. *J. Wood Chem. Technol.* **2005**, *25*, 187–202.
(13) Soderstrom, J.; Pilcher, L.; Galbe, M.; Zacchi, G. *Biomass Bioenergy* **2003**, *24*, 475–486.
(14) Schell, D. J.; Farmer, J.; Newman, M.; McMillan, J. D. *Appl. Biochem. Biotechnol.* **2003**, *105−108*, 69–85.
(15) Esteghlalian, A.; Hashimoto, A.; Fenske, J.; Penner, M. *Bioresour. Technol.* **1997**, *59*, 126–139.
(16) Lloyd, T.; Wyman, C. *Bioresour. Technol.* **2005**, *96*, 1967–1977.
(17) Thompson, D.; Chen, H.; Grethlein, H. *Bioresour. Technol.* **1992**, *39*, 155–163.
(18) Maloney, T. C.; Paulapuro, H. *Nordic Pulp Paper Res. J.* **1981**, *13*, 31–36.
(19) Menon, R.; MacKay, A. L.; Burgess, A. E.; Swanson, J. S. *J. Appl. Polym. Sci.* **1987**, *33*, 1141–1155.
(20) Araujo, C. D.; MacKay, A. L.; Whittall, K. P.; Hailey, J. R. *J. Magn. Reson., Ser. B* **1993**, *101*, 248–261.
(21) Topgaard, D.; Söderman, O. *Cellulose* **2002**, *9*, 139–147.
(22) Topgaard, D.; Söderman, O. *Langmuir* **2001**, *17*, 2694–2702.
(23) Stone, J. E.; Scallan, A. M. *TAPPI* **1967**, *50*, 496–501.
(24) Suurnakki, A.; Li, T. Q.; Burchert, J.; Tenkanen, M.; Viikari, L.; Vuorinen, T.; Odberg, L. *Holzforchung* **1997**, *51*, 27–33.
(25) Haggkvist, M.; Li, T. Q.; Odberg, L. *Cellulose* **1998**, *5*, 33–49.
(26) Li, T.; Henriksson, U. *Nordic Pulp Paper Res. J.* **1993**, *3*, 326–330.

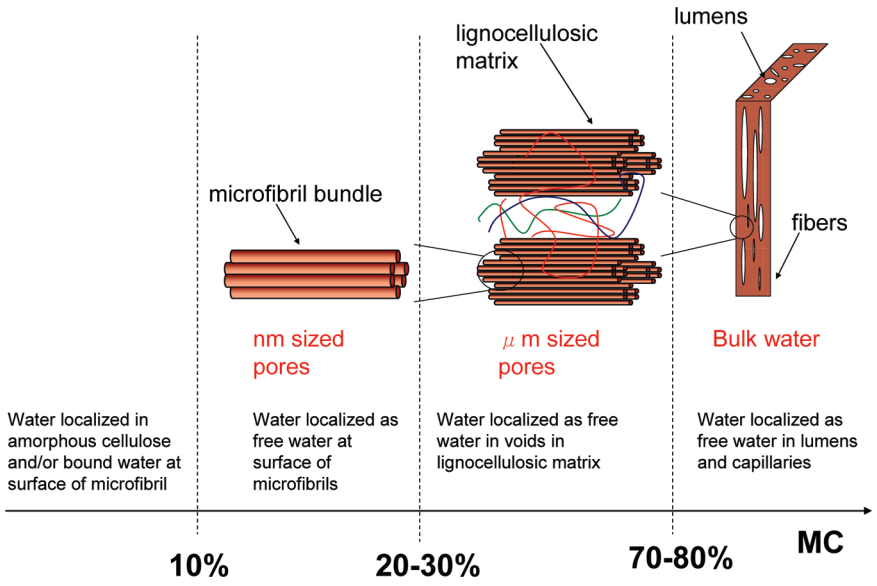

Figure 1. Schematic displaying the water pools or pore system that can be accessed via increasing moisture content (MC) in native biomass.

water pools or pores system studied.[19,27] The type and strength of this association, particularly in the cell wall material, are directly related to the ultrastructural and chemical state of the lignocellulose.[28,29] Though a pore system already exists in wood fibers, as pretreatment is performed, material is solubilized and removed from the biomass while also altering the ultrastructure state of the cellulose.[8] With either the pore size distributions, diffusion coefficients of the water, and/or the relaxation behaviors of the adsorbed water monitored, information about changes in the supramolecular or ultrastructure of lignocellulose can be inferred. This was done in an effort to further deconvolute the changes in lignocellulosic substrate characteristics upon pretreatment, to yield a better understanding of the mechanism involved and lead to a more deliberate pretreatment strategy to increase enzymatic activity, yield, and hydrolysis rate.

2. Experimental Section

2.1. Materials. Baseline *Populus* (*Populus trichocarpa x deltoides*) samples were harvested between 2007 and 2008 from area 0800 at Oak Ridge National Laboratory, TN. The samples were then shipped to the National Renewable Energy Laboratory (NREL) in Golden, CO for room temperature air drying, debarking, and size-reduction. The samples were stored in a freezer to maintain the moisture content and shipped to Georgia Tech upon request. The biomass was sized-reduced in a Wiley mill using a 20−80 mesh screen. Extractives were subsequently removed by placing 5 g of biomass into an extraction thimble in a Soxhlet extraction apparatus. The extraction flask was filled with 1:2 ethanol/benzene mixture (~150 mL) and then refluxed at a boiling rate which cycled the biomass for at least 24 extractions over a 4 h period.

2.2. Dilute Acid Pretreatment (DAP). Lignocellulosic samples were first prepared by presoaking, which was done at 25 °C while continuously stirring in a ~0.10 mol/m^3 dilute sulfuric acid solution at 5% dry extractive-free and size-reduced lignocellulosic solids (wt of solids/wt of suspension) for 4 h. The presoaked slurry was filtered to remove the solid material and washed with an excess of deionized (DI) filtered water. A mass of 2 g of the presoaked material (by dry mass) was transferred to a 4560 mini-Parr 300 mL pressure reactor with ~0.10 mol/m^3 H_2SO_4 solutions at 5% dry solids and was then sealed under ambient atmospheric conditions. The impeller speed was set to about 1.67 Hz, and the vessel was heated to 160 °C over ~25−30 min (at ~6 °C min^{-1}). The reactor was held at the pretreatment temperature ±2 °C (~650−690 kPa) for the specified residence time ±30 s (2.5, 5, 10, 20, and 60 min). The reactor was then quenched in an ice bath (~5 min) and the steam/atmosphere vented. The pretreated slurry was filtered to remove the solid material and washed with an excess of DI filtered water. The pretreated lignocellulosic samples were dried in the fume hood overnight at room temperature. Paramagnetic impurities generated during pretreatment from the surface of the reactor were removed by washing the solids with a 2 wt % aqueous solution of ethylenediaminetetraacetic acid (EDTA) and DI filtered water. All yields for biomass recovered after pretreatment ranged between 55 and 75% by mass of dry extractive-free and size-reduced lignocellulosic solids.

2.3. NMR Sample Preparation. Untreated and pretreated *Populus* was soaked in DI water or D_2O overnight to fully saturate the biomass. Saturated biomass samples were recovered by vacuum filtration on 0.25 μm nylon membranes. Samples were dried to the desired moisture content (MC) either by centrifugation or in a desiccator containing a saturated solution of either LiCl (relative humidity (RH) ~ 10%) and/or NaCl (RH ~ 75%) in DI water or D_2O over 48 h. Drying by centrifugation was achieved by first adding 2 g of anhydrous $MgSO_4$ to a centrifuge tube, along with a small piece of glass wool and additional nylon filter paper. The wood pulp was placed on top of the filter paper which rested on top of the glass wool. The tube was spun at 3000 rpm for a desired time. With dependence on the time of centrifugation, the MC could easily be adjusted between 40 and 80% with consistent variability of ~5% on successive trials. To further equilibrate the untreated and pretreated samples with respect to moisture content, after drying, the biomass was sealed in a zip-lock bag at room temperature overnight to equilibrate.

2.4. NMR Spectroscopy. ^{1}H NMR experiments on untreated and pretreated 20−80 mesh milled biomass pulp were performed on a benchtop low-field magnetic resonance analyzer (Maran 23 ultra), operating at a ^{1}H frequency of 23 MHz using a permanent magnet. A minimum of 500 mg of 20−80 mesh milled pretreated or untreated biomass pulp was measured in 10 mm NMR tubes at a constant temperature of 25 °C. The spin−spin

(27) Felby, C.; Thygesen, L. G.; Kristensen, J. B.; Jørgensen, H.; Elder, T. *Cellulose* **2008**, *15*, 703–710.
(28) MacKay, A.; Tepfer, M.; Taylor, I.; Volke, F. *Macromolecules* **1985**, *18*, 1124–1129.
(29) Froix, M.; Nelson, R. *Macromolecules* **1975**, *8*, 726–729.

relaxation times were determined using a standard Carr−Purcell−Meiboom−Gill (CPMG) sequence with 128 scans and τ = 100 us. Diffusion coefficients were measured using a pulse field gradient (PFG) simulated echo sequence with 128 scans, with a τ_1 = 16.7 ms, τ_2 = 83.3 ms, Δ = 0.1 s and taking 32 points varying δ between 0.0001 and 0.003 s. Spin diffusion experiments were conducted using a Goldman−Shen (GS) sequence having a T_2 filter of 0.5 ms, taking 32 points varying the mixing time between 5 and 10^6 μs. The relaxation delay for all sequences was 2 s, which was long enough based on the measurement of T_1.

^{2}H spin−lattice (T_1) NMR measurements were carried out on a Bruker DSX-300 spectrometer, operating at frequencies of 75.475 MHz for ^{2}H in a Bruker double-resonance MAS probehead at nonspinning conditions. The inversion recovery experiments utilized a 7 μs (90°) ^{2}H pulse, 14 μs (180°) ^{2}H pulse, 1 s recycle delay, and 128 scans. The NMR samples were prepared with milled pretreated or untreated biomass pulp using 7 mm cylindrical ceramic MAS rotors.

Inverse Laplace transforms (ILT) were accomplished by a Matlab 6 program written at Victoria University of Wellington (Wellington, New Zealand) by P. T. Callaghan to process one- and two-dimensional ASCII data measuring either diffusion or relaxation characteristics of heterogeneous proton systems. This program is based on unconstrained regularization, non-negative least squared fit, and singular value decomposition algorithms. The routine was tested using a series of multiexponential and stretched-exponential functions of varying component weights, widths, and characteristic decay times demonstrating fairly good accuracy, resolution, and stability in the corresponding distributions produced. To assess the effect of noise, relaxation curves were generated using a multiexponential function and each data point was allow to increase or decrease by a maximum of 10% of its only value. The particular variance at each data point was controlled by a random number generator to simulate a randomly noisy relaxation curve. Again resulting transforms produce reliable peak intensities, positions, and widths.

2.5. Nitrogen Sorption Isotherms. Nitrogen adsorption measurements at 77 K were performed on a Gemini 2370 surface area analyzer (Micromeritics Instrument Corp., Norcross, GA). Total pore specific surface area and volumes were determined using a multipoint BET method. Biomass samples were prepared based on a solvent exchange method which shows minimal pore collapse upon drying.[30,31] The biomass samples were soaked overnight in DI water and filtered. The water saturated samples were then soaked for 4 h each in 25/75 acetone/water, followed by 50/50 acetone/water, and 75/25 acetone/water solutions before finally filtering allowing the biomass to soak in acetone overnight. The biomass was recovered by filtering and allowed to again soak in cyclohexane/acetone mixtures and cyclohexane following the same solvent exchange procedure above. The biomass was then filtered and allowed to dry in the hood for 8 h, dried under reduced atmosphere at 40 °C overnight, and further dried and degassed under N_2 purge at 40 °C for 1 h.

3. Results and Discussion

A particular useful tool for increasing the effectiveness of downstream processing of a biomass energy crop is dilute acid pretreatment.[3] In an effort to better understand the changes occurring within biomass during DAP, various ^{1}H and ^{2}H NMR experiments were conducted on untreated and pretreated *Populus* at various controlled moisture contents (MC)s. The later point is particularly important because based on the MC various pore systems as described in Figure 1 can be accessed and subsequently probed. The *Populus* samples were pretreated varying the experimental parameter of time to not only achieve controlled variations but to also understand the origin and extent of those variations due to recalcitrance within the structure of lignocellulosics. Our initial studies examined untreated and pretreated *Populus* using ^{1}H CPMG experiments (~60% MC) to probe T_2 relaxation of absorbed water. This was followed by treatments of data from ^{2}H T_1 (~25% MC) and ^{1}H GS experiments (~60% MC) generating conclusions about pore size distributions and the shift upon pretreatment. The final set of studies were devoted to PFG experiments (~60% MC) studying the change in self-diffusive behavior of adsorbed water, which can be related to pore tortuosity.

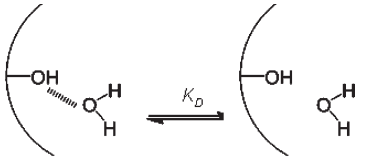

Figure 2. Schematic displaying the exchange between free and bound water with the pores of a biomass sample.

3.1. Spin−Spin Relaxation. Felby et al.[27] used time domain (TD) low-field NMR to study the different states and locations of water pools within the lignocellulose matrix and how those water pools changed with enzymatic hydrolysis. They determined the state and location of water pools could be associated with structural changes in cellulose. Three water pools or pore systems were observed and attributed to pores with (1) water associated with cellulose fibril surfaces, (2) water in the cell wall matrix, and (3) capillary water in the lumens and between fibers.[27] Similarly, in this study we used a CPMG sequence with TD NMR to study the different states and locations of water pools within the lignocellulose matrix as a function of DAP, specifically with increasing pretreatment time.

Changes in the relaxation behavior of a probe molecule occurs within porous media because of two major mechanisms: (1) residual dipolar coupling due to anisotropic reorientation of water resulting from interactions with the pore surface and pore confinement and/or (2) exchange of water protons between the bulk and bound water phases by chemical exchange.[43−45] Figure 2 illustrates a depiction of this chemical exchange which is defined by a dissociation constant, K_D, and directly related to the pore surface chemistry. The exchange process is assumed to be under fast conditions, and therefore the observed relaxation behavior of water within a particular pore is a weighted average of states (instead of some spatial gradient of relaxation rates), approximated by the following equation:

$$\frac{1}{T_{2\mathrm{obs}}} = \frac{X_{\mathrm{free}}}{T_{2\mathrm{free}}} + \frac{X_{\mathrm{bound}}}{T_{2\mathrm{bound}} + \tau_{\mathrm{bound}}} \quad (1)$$

where $T_{2\mathrm{obs}}$ is the observed relaxation constant of a particular pore, and $T_{2\mathrm{free}}$ and $T_{2\mathrm{bound}}$ are the relaxation constants related to free and bound water, respectively. τ_{bound} is the average lifetime in the bound state which is typically much shorter than $T_{2\mathrm{bound}}$. $T_{2\mathrm{free}}$ will be strongly responsive to the solution properties inherent to the probe molecule including temperature, impurities, etc. $T_{2\mathrm{bound}}$ on the other hand will be dominated by strong intramolecular associations at the liquid/solid surface, proportional to K_D. If the pore system was to grow, X_{free} and X_{bound} would also change as they are proportional to the surface area to volume ratio of the

(30) Stone, J.; Scallan, A. *J. Polym. Sci., Part C: Polym. Symp.* **1965**, *11*, 13–25.
(31) Haggkvist, M. *Nordic Pulp Paper Res. J.* **1998**, *13*, 292–298.

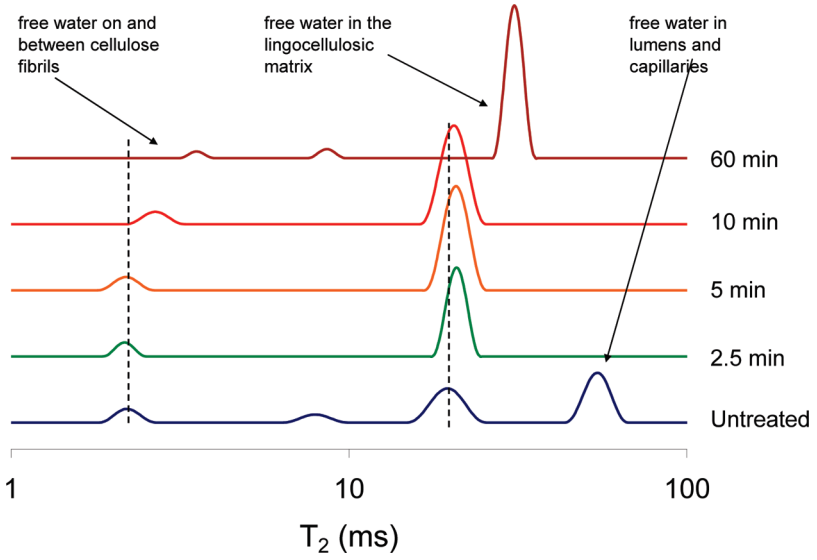

Figure 3. Distribution of spin−spin relaxation times of absorbed water within untreated and pretreated *Populus* biomass (pretreated in 0.10 M H_2SO_4 at 160 °C for various residences time) produced via ILTs of CMPG T_2 experiments at a moisture content of 60 ± 3%. The vertical dotted lines serve to visually demonstrate shifts in the peak position.

pores.[43−45] Considering this, using T_2 or T_1 relaxation of water to probe the relative sizes and type of interactions of water within pores of biomass seems particularly reasonable.

The CPMG experiment results in a very typical T_2 decay profile of water within untreated *Populus* at a MC of ~60%. The decay is clearly exponential-like in nature; however, discerning whether the decay represents a single exponential decay or multiple heterogeneous decays is visually difficult to determine. Upon application of various spin−spin relaxation models the fit residuals did indicate the decay to have at least two exponential components.

The analysis of multicomponent T_2 profiles can be difficult when utilizing any one particular model especially when there is a wide distribution of unknown decay constants, decay constants with very similar values or appreciable noise or baseline effects. One method to resolve this, while also visually depicting any change in T_2 relaxation, is to extract the distribution of relaxers or exponential decays from the T_2 data using an inverse Laplace transform (ILT) or more accurately a series of unconstrained all-positive-coefficient least-squares fits.[27,32] There is an inherent concern involved in using ILT routines particularly from noisy data sources. However an absolute ILT solution is not required here, but instead the power of this analysis relies on qualitative comparisons of peak intensities, positions, and widths among similar samples from the same feedstock modified by the same process in an increasingly severe way. The ILT routine in this case should be able to detect differences in the relaxation distribution's population, position, and width when those differences are above some critical threshold even when there is some ambiguity in the transformation solutions. Care was taken to properly test the ILT routine as described in the Experimental Section to ensure the validity of this particular analysis.

ILTs were used in this study and can be seen in Figure 3 as a stack plot of the distribution of spin−spin relaxation times of absorbed water within untreated *Populus* and *Populus* dilute acid pretreated for 2.5, 5, 10, and 60 min.

In systems with few proton sources of interest such as H_2O filled biomass, using TD NMR to analyze the T_2 relaxation is ideal.[27,32,33] The T_2 distribution for the untreated sample indicates at least three pools of water exist within the lignocellulose at 60% MC, as similarly depicted in Figure 1. The peak centered around 2 ms is assigned to "free" water on and between cellulose fibrils, spatially localized within the fibril bundle. The relatively fast relaxation times suggest this pool of water is on average less mobile, having less degrees of freedom. This can be interpreted as meaning the water in that pool is either within a much more confined volume, having a lower X_{free}/X_{bound} ratio and/or increased interactions with the lignocellulose substrate sufficiently retards the molecular dynamics of the water. Somewhat further along the T_2 time axis, at ~20 ms, another peak of much higher relative intensity is observed and attributed to "free" water within voids of the hemicellulose−lignin matrix encasing the cellulose bundles. The increase in relaxation times relative to the first peak mostly likely is due to the fact that pores in this region are on the order of 10−100 times larger than those associated with the first water pool. The third peak at ~60 ms represents the slowest decaying component of the water in the *Populus* and is associated with "free" water in lumens and fibers capillaries. The peak assignments of water to the three previously mentioned locations are very similar in the average T_2 value to those assignments done by Menon et al. on softwoods and Elder et al. on char of hardwoods, seemingly supporting the above conclusions.[19,32] Lastly, the relative integrated intensity of the first and second peaks are ~1:4. This ratio directly corresponds to previously mentioned literature results on the structure of cellulose fiber walls during drying, which suggest ~10% of biomass moisture regain is localized on and between fibril bundles and ~40% in the lignocellulosic matrix.

The vertical dotted lines in Figure 3 are there to serve as reference points intended to help visually indicate the relaxation time shifts occurring upon pretreatment. Most notably, the third and slowest relaxing peak disappears after the pretreatment temperature ramp-up and initial 2.5 min of

(32) Elder, T.; Labbe, N.; Rials, T. *Biomass Bioenergy* **2006**, *30*, 855–862.

(33) Blumich, B.; Anferova, S.; Sharma, S.; Federici, C. *J. Magn. Reson.* **2003**, *161*, 204–209.

reaction. This is interpreted as the destruction of this pore system. The other two peaks show slight shifting in T_2 times to longer values at both 2.5 and 5 min of pretreatment, the fastest relaxing water pool or first peak shows a sufficient increase in T_2 times after 10 min and the intermediate relaxing water pool or second peak shows a signficant shift after 60 min. Those two peaks show a shift in T_2 times to longer relaxation or a more mobile state, displaying relative intensity increases that also indicate the population of water in the intermediate relaxing water pool increases with pretreatment.

The observe changes in Figure 3 mainly suggest an increase in porosity or pore size, as pretreatment disrupts the lignocellulosic supramolecular structure more water can adsorb into those regions. An alternative explanation for the observed shifts in T_2 times could be related to the change in pore surface chemistry. As pretreatment proceeds, hemicellulose is removed and the pore surface becomes lignin rich. The shift toward a more hydrophobic surface would decrease interactions of water with the lignocellulose substrate, which would increase the motion of water within the pores. However because the majority of the hemicellulose removal and lignin enrichment occurs within the first 2.5 min of pretreatment and little change in the T_2 times are detected, the later affect seems to be minor. On the basis of this, pore expansion seems to be particularity significant in the behavior of the second peak, associated with pores in the hemicellulose–lignin matrix, which shows the largest change in peak appearance with pretreatment.

3.2. Pore Size Distributions. It is well-known liquid molecules near a solid surface will have different relaxation profiles from that of the bulk liquid because of interactions at the solid–liquid interface.[25,26,34−38] Consequently, in porous systems that contain water, the observed average T_1 time of the water is influenced by and proportional to the surface area to volume ratio of the pores. Models describing this change in relaxation have been generated based on a two-component system, under fast exchange conditions where the observed T_1 is the weighted sum of relaxation times of free and surface-associated water.[35,39] This model has been extended to describe a continuous system and was used in this paper to relate T_1 relaxation behavior of adsorbed water to pore distribution information.

Work detailing the effect of drying on the structure of the cell fiber wall not only demonstrated the usefulness of ^{2}H NMR relaxation as a method to investigate pore size and pore size distribution but also clearly indicates moisture content of a fiber can greatly influence any measurement conducted on the pore system. Though this may be true, Li et al. also found that whether the samples were dried via pressing or centrifugation the resulting pore size distribution were almost identical as along as the MCs were similar.[26] Therefore, special care was taken in this study to equilibrate all samples to achieve small variations in MC. Also, although both ^{2}H and ^{1}H T_1 relaxation profiles could be used to determine pore sizes in biomass, D_2O has a $I = 1$ spin possessing a quadrupolar moment. As a result, ^{2}H relaxation mechanisms are mainly intramolecular in nature, not affected by paramagnetic impurities, giving rise to a more accurate measurement of pore surface area to volume ratio and therefore is the nucleus of interest in this section of the study.[25,26]

Written in terms of pore surface area (S_p) and pore volume (V_p), the observed average spin–lattice rate $\langle T_1 \rangle$ within a water filled pore can be described by

$$\left\langle \frac{1}{T_1} \right\rangle = \frac{1}{T_{1F}} + \frac{\left(\frac{1}{T_{1B}} - \frac{1}{T_{1F}}\right)\lambda S_p}{V_p} = \alpha + \frac{\beta}{r_p} \qquad (2)$$

where T_{1F} and T_{1B} are the spin–lattice rates of free and surface-associated (bound) water, respectively, and λ represents the thickness of the surface-associated water layer. With rearrangement of this equation, the pore radius, r_p, is defined as a volume over an area and ultimately related to the physical constants $\alpha = 1/T_{1F}$ and $\beta = 2\lambda(1/\{T_{1B} - 1/T_{1F}\})$.[25,26] Determining α can be easily accomplished via direct spin–lattice measurements of bulk water. Upon this measurement of bulk D_2O, α was found to be 2.48 s^{-1}. However the unknown quantities of λ and T_{1B} make evaluating β somewhat more difficult.

β is a physical constant that describes the interactions between the liquid probe molecule and the solid surface. Once determined for a particular pore system, the relationship in eq 2 can be used to solve for r_p without any knowledge of S_p, V_p, λ, or T_{1B}. Li et al. describes three methods to determine β for a particular pore system.[26] The method used in this paper utilizes a gravimetrically obtained nitrogen adsorption/desorption isotherm and multipoint (Brunauer–Emmett–Teller) BET method to determine specific pore surface area (S_o) and specific pore volume (V_o) of a biomass sample. β can then be calibrated for samples of similar surface–liquid interactions by

$$\beta = \frac{2V_o}{S_o}\int_{T_{1min}}^{T_{1max}} \frac{P(T_1)}{T_1}\,dT_1 \qquad (3)$$

where $P(T_1)$ is the population of nuclei with the spin–lattice rate of T_1.[25,26]

To obtain S_o, the initial portion of the nitrogen adsorption isotherms were analyzed by the BET equation:[40,41]

$$\frac{1}{W\left(\frac{p_s}{p}\right) - 1} = a\left[\frac{p}{p_s}\right] + b \qquad (4)$$

where p_s/p is the nitrogen partial pressure and W is the weight of adsorbed nitrogen. On the basis of eq 3, slope (a) and y-intercept (b) values can be used to determine the weight of a monolayer of nitrogen within the pore system, $W_m = 1/(a+b)$. W_m is related to S_o through

$$S_o = \frac{W_m N_A A_{cs}}{M} \qquad (5)$$

where N_A is Avogadro's number, A_{cs} is the cross-sectional area of a nitrogen molecule (16.2×10^{-16} cm^2),[40] and M is the

(34) Gallegos, D.; Munn, K.; Smith, D.; Stermer, D. *J. Colloid Interface Sci.* **1987**, *119*, 127–140.
(35) Gallegos, D.; Smith, D.; Brinker, J. *J. Colloid Interface Sci.* **1988**, *124*, 186–198.
(36) Gallegos, D.; Smith, D. *J. Colloid Interface Sci.* **1988**, *122*, 143–153.
(37) Glaves, C.; Frye, G.; Smith, D.; Brinker, C.; Datye, A.; Ricco, A.; Martin, S. *Langmuir* **1989**, *5*, 459–466.
(38) Glaves, C.; Smith, D. *J. Membr. Sci.* **1989**, *46*, 167–184.
(39) Xu, Y.; Araujo, D.; MacKay, A. L.; Whittall, K. *J. Magn. Reson., Ser. B* **1996**, *110*, 55–64.
(40) Hansen, T. *Mater. Struct.* **1986**, *19*, 423–436.
(41) Fagerlund, G. *Mater. Struct.* **1973**, *6*, 239–245.

Table 1. Average Spin−Lattice Times of Absorbed D_2O within Untreated and Pretreated *Populus* Biomass (Pretreated in 0.10 M H_2SO_4 at 160 °C for Various Residences Time) at a Moisture Content of 24 ± 5% Measured by a Inversion Recovery Sequence

sample	T_1 (ms)
untreated	23.9
5 min	27.8
10 min	32.0
60 min	36.3
free H_2O	402.1

molar mass of a nitrogen molecule. V_o was also obtained from the nitrogen adsorption isotherm by

$$V_o = \frac{W_{p/p_s=1}}{\rho} \quad (6)$$

where ρ is the density of liquid nitrogen and $W_{p/p_s=1}$ represents the amount of nitrogen in a gram of biomass upon fiber saturation. β for a D_2O filled untreated *Populus* biomass was found to be 52.2 nm s^{-1}, which is close to those listed in the literature for a similar system.[25,26] The β parameter was recalculated for each pretreated sample based on the acquired nitrogen adsorption isotherm and T_1 relaxation distribution for that sample, which allowed for the comparison between samples of highly varying pore surface properties.

The spin−lattice relaxation profile of absorbed D_2O within untreated and pretreated *Populus* biomass at a moisture content of ~60% was recorded and found to be very characteristic of the type of curve resulting from an inversion recovery experiment. With the application of a model $[M(\tau)/M_0 = 1 - (2\exp(-\tau/T_1))]$ to the relaxation curves, an average T_1 time based on the signal intensity change seen in an inversion recovery experiment was determined and tabulated in Table 1. The values in Table 1 suggest untreated *Populus* has the highest surface area to volume ratio as the surface-associated water T_1 weights, with the observed average T_1 the greatest. As the sample is pretreated, the average T_1 increases indicating relatively less surface-associated water is in the biomass as pretreatment proceeds and is interpreted as pore expansion. The average pore radius, r_p, can be determined using the constants α and β in eq 1 on the observed average T_1 values in Table 1, or a pore size distribution can be generated by applying α, β, and eq 2 to an ILT of the T_1 relaxation, which produce distributions of T_1 relaxation for the D_2O within the biomass pore system.

The resulting pore size distributions are shown in Figure 4 for untreated and pretreated *Populus* biomass at a MC of 24 ± 5%. At this MC, D_2O should be in the nanometer-sized pores, localized on and between cellulose fibrils, minimizing any deuterium oxide on external surfaces or within the larger pore systems. Figure 4 displays not only a systematic shift in pore radius to larger values but also a relatively significant broadening of the pore distributions and decrease in normalized intensity with increasing pretreatment time. This would suggest that the observed shift in pore radius is due to existing pores within the system expanding rather than the generation of new pores.

By integration of the area under the distributions, a number-average radius was calculated and then used to produce total pore surface area and volume changes due to pretreatment. These values are listed in Table 2 and indicate that the surface area associated with pores within the cellulose fibril bundles increase by a factor of 3.5 and pore volume by a factor of 6.5

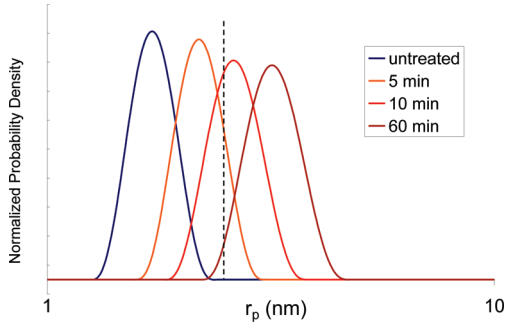

Figure 4. Pore size distribution based on D_2O adsorption and ^2H T_1 relaxation for untreated and pretreated *Populus* biomass (pretreated in 0.10 M H_2SO_4 at 160 °C for various residences times) at a moisture content of 24 ± 5%. The vertical dotted line represents 26 Å, the minimal pore radius for cellulase.

Table 2. Ratio of Pore Volume and Surface Area As *Populus* Biomass Is Pretreated in 0.10 M H_2SO_4 at 160 °C for Various Residences Time at a Moisture Content of 24 ± 5%

sample	$pore_{SA}/pore_{SA}^{Un}$	$pore_{Vol}/pore_{Vol}^{Un}$	$pore_{Dia}/pore_{Dia}^{Un}$
5 min	1.6	2.0	1.3
10 min	2.3	3.5	1.5
60 min	3.5	6.5	1.9

after 60 min of DAP. A vertical dotted line in Figure 4 again serves as a reference point for peak comparison but also represents 26 Å, the minimal pore radius for cellulase accessibility.[8] Therefore, according to Figure 4, the pores in native *Populus* are on the order, if not slightly smaller, than the size for cellulase accessibility and the detected changes in their sizes due to pretreatment can significantly affect the relative amount of cellulase present in the biomass and its subsequent activity. As clearly demonstrated in the plot, the untreated biomass has relatively no portion of it is pore distribution larger that 26 Å, as pretreatment proceeds the distribution shifts, until the distribution at 60 min of DAP shows a pore size distribution in which the majority of the pores are large enough to give cellulase access. As a consequence, the observed increases in cellulase activity with pretreatment commonly observed throughout the literature[12−16] are at least in part due to changes in the pore system on and between cellulose fibrils.

The changes within the complete pore system for biomass upon pretreatment are not limited to the water pool or pores association with fibril bundles. One main goal of pretreatments is the removal of hemicellulose, which should greatly affect the size of the water pool or pores association with the lignocellulosic matrix, described as micrometer-pores. To probe the changes in that system of pores, H^2 spin−lattice relaxation experiments were conducted on untreated and pretreated *Populus* biomass at a MC of ~60%. The resulting distribution was not able to resolve the micrometer-sized pores. These types of relaxation experiments seem to only detect pores up to the radius of ~100 nm due an inability by any model or transform to resolve differences in relaxation times of larger pores from that of bulk water. Essentially the proportional of bound water is so low in these pores that the additional relaxation due to chemical exchange with bound water becomes negligible.

3.3. Cross-Relaxation. Goldman−Shen (GS) spin diffusion or cross-relaxation experiments use a T_2 filter to selectively place magnetization within the water of filled biomass pores. A mixing time delay allows magnetization to transfer from

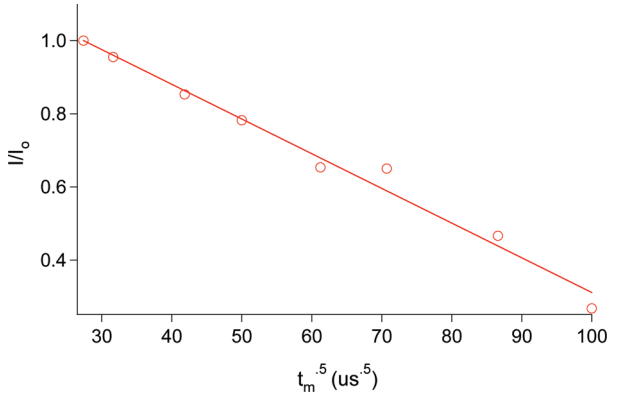

Figure 5. Initial portion of the experimental curve from a Goldman–Shen experiment on untreated *Populus* biomass at a moisture content of ~60%.

the water into the cellulose; therefore, information about the rate of magnetization transfer between the water and cellulose can be extracted by conducting the spin diffusion experiment as a function of mixing time.[22,42] With the neglect of longitudinal relaxation effects, the rate of magnetization transfer is proportional to the surface area to volume ratio in water filled domains. On the basis of work done on polymer blends and on copolymers, a relationship for the initial rate of signal attenuation of a GS experiment is related to the size of the water filled pores:[42]

$$r_p = \frac{3}{\sqrt{\pi}}\sqrt{D_{eff} t_m^{s,0}} \quad (7)$$

where D_{eff} is the effective spin diffusion coefficient of wood and water and $t_m^{s,0}$ is the x-intercept of a linear initial-rate approximation as seen in Figure 5. Figure 5 shows the GS experiment on untreated *Populus* biomass at a MC of ~60%, and the solid line represent the linear fit to the initial rate of decay. Unfortunately, spin diffusion coefficients are difficult to measure or even estimate, so eq 7 can only be used to qualitatively measure the magnitude of the observed pore expansion.

The $\sqrt{t_m^{s,0}}$ was 127, 227, and 272 μs for the untreated *Populus* and *Populus* pretreated for 2.5 and 5 min, respectively. On the basis of eq 7 and the results above, this corresponds to an increase in pore surface area by a factor of 3.2 and 4.6 and the pore volume by a factor of 4.4 and 9.3 after 2.5 and 5 min of DAP. These increases, though very similar, are slightly larger than those observed via H^2 spin–lattice relaxation experiments on untreated and pretreated *Populus* biomass, seen in Table 2.

This difference could be due to the additional pore expansion occurring in the lignocellulosic matrix not detected by the H^2 spin–lattice relaxation experiments. However, cross-relaxation can also occur due to chemical exchange between protons on the pore surface of the biomass and water. Therefore, the changing pore surface chemistry due to pretreatment may also affect the rate of magnetization transfer. There is no question that these types of GS experiments probe the type and extent of substrate alterations occurring during pretreatment; however, to completely extract the origins of the changes observed in cross-relaxation rate (pore expansion versus chemical exchange), which seem beyond the scope of this study, these experiments must be done as a function of temperature. Nevertheless, though the magnitude of change due to the changing pore surface chemistry is unknown, it is known that the pore surfaces will be enriched with lignin essentially decreasing chemical exchange and the relative cross-relaxation rate related to the pore surface area to volume ratio with pretreatment residence time. It therefore becomes reasonable to suggest the results from the untreated sample represents some lower pore size limit while the result at 5 min represents some upper limit. On the basis of the close correlation with the T_1 relaxation experiments, these GS results seem to be a reasonable alternative to depicting the changes happening in both the microfibril bundles and lignocellulosic matrix, while at a minimum qualitatively supporting the earlier results and subsequent conclusions.

3.4. Self-Diffusion. One property of the solvent probe molecule that can be gathered in a fairly straightforward manner by direct NMR measurement is the apparent self-diffusion (D_s) coefficient.[21,22] This can be done using a pulse field gradient (PFG) sequence. The resulting signal attenuation occurring during the experiment can be related to

$$\frac{I}{I_o} = \exp\left[-(\gamma G\delta)^2 D_s\left(\Delta - \frac{\delta}{3}\right)\right] \quad (8)$$

where G is the gradient strength, δ is the amount of time the gradient is applied, and Δ is the delay between the application of the gradients. By systematically varying either G, δ, or Δ the D_s of a system can be determined. Also, with the use of a well-defined $(\Delta-\delta/3)$ interval or period of observation, PFG experiments can probe the diffusion of a molecule over various length scales. The larger the interval, the longer the technique "observes" or the larger the root-mean distance of observation in which the diffusion coefficient is determined over.

Again, instead of solving for an average D_s and fitting a single or multicomponent diffusion model to the attenuation, the diffusion data was processed using an ILT routine. The resulting D_s distribution of water adsorbed in untreated and pretreated *Populus* biomass at a moisture content of ~60% is shown in Figure 6. The vertical dotted line in Figure 6 represents the bulk self-diffusion coefficient (D_o) of water, which is 2.27×10^{-9} m^2 s^{-1} and serves as a line of reference to indicate distribution shifts in the stack plot. The D_s distribution for the untreated sample indicates there are at least two resolvable D_s of water within the lignocellulose. One peak is centered around 2.09×10^{-9} m^2 s^{-1}, very close to that of bulk water while the other peak is observed at ~5.49×10^{-10} m^2 s^{-1}, well within the range of diffusion coefficients found for water within biomass by Topgaard et al.[21,22] The peak of slower diffusion most likely is related to water within the biomass pore systems. As pretreatment proceeds, Figure 6 indicates the D_s distribution of water within the biomass pore system shifts to slower diffusive motion.

This result initially seems counter-initiative. However, with the use of relationships defined through electrical conductivity and applied to diffusion of water through porous materials by Latour et al.,[22,43] the above results are consistent with theory and become tremendously informative. In a PFG experiment on porous material filled with a fluid in which the $(\Delta-\delta/3)$ interval or period of observation is very

(42) Mellinger, F.; Wilhelm, M.; Spiess, H. W. *Macromolecules* **1999**, *32*, 4686–4691.
(43) Latour, L.; Kleinberg, R.; Mitra, P.; Sotak, C. *J. Magn. Reson., Ser. A* **1995**, *112*, 83–91.
(44) Belton, P. S. *Macromolecules* **1991**, *24*, 2944–2950.
(45) Paradossi, G.; Cavalieri, F. *Carbohydr. Res.* **1997**, *300*, 77–84.

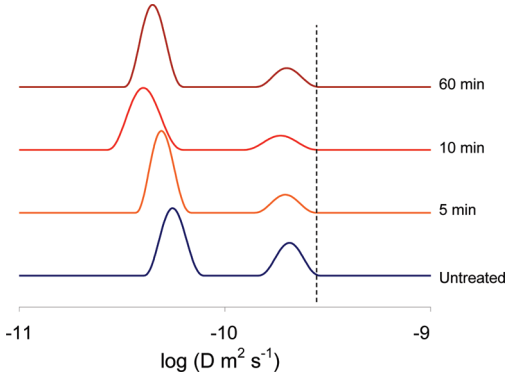

Figure 6. Diffusion coefficient distribution of water adsorbed in untreated and pretreated *Populus* biomass (pretreated in 0.10 M H_2SO_4 at 160 °C for various residences times) at a moisture content of 60 ± 3%. The vertical dotted line represents the self-diffusion coefficient of free water.

small, the apparent D_s will be close to that of the bulk fluid or somewhat similar to that of D_o. As the $(\Delta-\delta/3)$ interval or period of observation is increased, the apparent D_s will remain relatively unchanged until, at some point, the root mean distance of observation approaches the size of the pores or length scale of confinement. At that point, the apparent D_s should suddenly decrease with an increase in the $(\Delta-\delta/3)$ interval or period of observation. Again, as the $(\Delta-\delta/3)$ interval or period of observation is further increased at some point, the root mean distance of observation will be much larger than the size of the pores or length scale of confinement. At that point, the apparent D_s should level-off again, denoted as D_∞.[22] Essentially, D_s has a decreasing sigmoidal relationship with an increase in the $(\Delta-\delta/3)$ interval or period of observation with D_o as the upper limit and D_∞ as the lower limit.

The apparent D_s for untreated *Populus* was measured as a function of increasing the $(\Delta-\delta/3)$ interval or period of observation, and the onset of the transition from D_o to D_∞ was found at a period of observation of ~0.5 s with an apparent D_s of 8.32×10^{-10} m^2 s^{-1}. With the use of a relation between the apparent D_s over a defined observation interval $(\Delta-\delta/3)$, a one-dimensional root-mean squared distance can be determined.[22]

$$\sqrt{\langle z^2 \rangle} = \sqrt{2\left(\Delta - \frac{\delta}{3}\right) D_s} \qquad (9)$$

If the root-mean squared distance is calculated at the onset of the transition from D_o to D_∞, the average distance over which a water molecule diffuses before reaching the pore walls or length scale of confinement can be established. On the basis of the relationship in eq 9 and data on the transition from D_o to D_∞, the average unrestricted diffusional path length of water in untreated *Populus* is ~30 μm (correlates with lignocellulosic matrix pore dimensions).

With the use of relationships defined through electrical conductivity, inferences can be made about the porous media tortuosity (T), which describes the interconnectivity of a pore system, and this relationship can be defined by[22]

$$\frac{1}{T} = \frac{D_\infty}{D_o} \qquad (10)$$

Taking the average diffusion coefficient, as seen in Figure 6, from the D_s distributions of water within the biomass pore system as D_∞, the tortuosity increases relative to the untreated sample by ~40% at 5 and 10 min of pretreatment and by ~70% after 60 min of pretreatment. The results of the analysis using eq 9 suggest the pores within the probed water pool or pore systems are becoming more interconnected and tortuous with pretreatment. Also, this along with the average pore diameter of untreated *Populus* calculated above indicates these PFG experiments (at ~60% MC) are particularly sensitive to water localized in the hemicellulose−lignin matrix (corresponding to micrometer-pores). This makes sense considering pores or a root-mean squared distance having nanometer-sized dimensions observed under the smallest $(\Delta-\delta/3)$ interval used in this set of PFG experiments (~0.01 s) would have a diffusion coefficient on the order of 10^{-15} m^2 s^{-1}, well outside the lower bound for the ILT routine.

4. Conclusions

The effect of DAP on *Populus* biomass was studied using three techniques: (1) TD NMR using a CPMG sequence to probe T_2 relaxation of absorbed water, (2) ^{2}H NMR relaxation as a method to investigate the pore size and pore size distribution, and (3) PFG experiments to investigate the self-diffusive behavior of water adsorbed within the biomass. The T_2 measurements can be used to show how the nature and magnitude of cellulose−water interactions change during DAP. Water, which can be found spatially localized on and within cellulosic microfibrils, is described to exist also as capillary water in the lumen or between fibers and within the lignocellulosic matrix. The ILT distributions of T_2 relaxation times demonstrate not only a shift in T_2 times to longer relaxation or a more mobile state but also indicate the population of water with longer relaxation times increase. This suggests during pretreatment the lignocellulosic structure of *Populus* begins to breakdown and loosen, particularly within the lignocellulosic matrix. ^{2}H T_1 NMR was used to generate pore size distributions, and the results indicate that pore expansion in cellulose fibers occur during pretreatment. Specifically, pores within fibril bundles enlarge such that appreciable amounts of enzyme have access to cellulose microfibrils. GS spin diffusion experiments seem to support the T_1 experiments while also indicating pores within the lignocellulosic matrix undergo considerable expansion also. Diffusion experiments suggest an increased tortuosity with pretreatment.

Acknowledgment. This work was supported and performed as part of the BioEnergy Science Center. The BioEnergy Science Center is a U.S. Department of Energy Bioenergy Research Center supported by the Office of Biological and Environmental Research in the DOE Office of Science. In addition, we wish to thank the reviewers for their insightful comments. A special thanks goes to P. T. Callaghan for access to the inverse Laplace transform program.

Note Added after ASAP Publication. There were errors in the version published ASAP September 20, 2010. An sentence was deleted at the end of section 3.1; the corrected version reposted on September 24, 2010.